Ground-penetrating radar inspection of Subsurface Historical Structures at the Baptism (El-Maghtas) site, Jordan

[(1)]AbdEl-Rahman Abueladas*, [(1)]Emad Akawwi

[(1)]Surveying and Geomatics Department, Faculty of Engineering, Al-Balqa Applied University, Al-Salt 19117, Jordan.

** Corresponding author e-mail: aabueladas@bau.edu.jo, Tel: +962 0791709827, Fax:+962 5 3530465*

Abstract

The Baptism (El-Maghtas) site is located to the north of the Dead Sea on the eastern bank of the Jordan River. Previous archeological excavations in the surrounding area have uncovered artifacts that include the location was home to "John the Baptist," who lived and preached in the early 1st Century AD and is known for baptizing Jesus. Archeological excavations have revealed walls, antiquities, and ancient water systems that include conduits, pools, and ancient pottery pipes. A Ground Penetrating Radar (GPR) survey was carried out at select locations along parallel profiles using a Subsurface Interface Radar System (Geophysical Survey Systems Inc. SIRvoyer-20) with 400 MHz or 900 MHz mono-static shielded antennas in order to locate archaeological materials at shallow depths. The GPR profiles revealed multiple subsurface anomalies across the study area. At the John the Baptist Church site buried wall were detected along the profiles, and at the pool site the survey delineated several buried channels. GPR data also confirmed the extension of an ancient pottery pipe at Elijah's Hill site through the production of a clear diffraction hyperbola anomaly related to the ancient pottery pipe that could be discriminated from the 2D profiles. The GPR data was displaced using 3D imaging to define the horizontal and vertical extent of the pipe.

Keywords: Jordan River, Baptism, Archaeological remains, pottery pipe, Ground Penetrating Radar.

1 Introduction

Locating an archeological site that contains buried artifact, and antiquities has traditionally methods such as coring, foretelling, and shovel testing, which are time-consuming and labor intensive procedures that can lead to significant waste of time and expense. Ground-penetrating radar (GPR) is a unique high-resolution tool that offers a solution to these problems (Vaughan 1986).

GPR uses electromagnetic (EM) waves with frequencies of 10-1000 MHz to picture subsurface soil and structure. It has become an accepted method for use in various fields, including archaeology, geology, engineering and construction, environmental fields, and forensic science (Neal 2004). The advantage of using EM waves with relatively short wavelengths lies in the ability to map small objects at shallow depth. This GPS methodology has been successfully utilized to locate antiquities in urban and arid settings (Vaughan 1986; Sternberg and McGill 1995; Cacione et al. 1996; Basile et al. 2000, Ronen et al., 2018) and has proven to be an efficient method for identifying areas with the highest potential for successful excavation (Cacione 1996).

Additionally, GPR data presentations can play a significant role in archaeological inspections since they provide a visual representation of the site, including the size and depth of any subsurface anomalies (Basile et al. 2000).

The main objective of this study to carry out a ground-penetrating radar (GPR) survey, which is a non destructive and non-invasive method of obtaining information about the existence of archaeological features in shallow subsoil and to image the extension of a partially excavated ancient pottery pipe. The Baptism Site is situated approximately eight kilometers from the northern corner of the Dead Sea on the eastern bank of the Jordan River (Fig. 1).

Figure 1

The site is located in an arid environment where a large number of archaeological remains of various age, and size are located in variable geological–archaeological media (Eppelbaum et al., 2010). Soils at the site are complex, and in some locations vegetation factors complicate the accessibility of GPR survey (Eppelbaum and Khesin, 2001; Eppelbaum et al., 2010.

The GPR survey was carried out at three different sites to identify any shallow anomalies

2 Historical Background

The Baptism (El-Maghtas) site is a prehistoric area in Jordan Valley, about 50 km from Amman in western Jordan, settlements within El-Maghtas known as Bethany in the place where John the Baptist lived in the time of Christ, making El-Maghtas one of the most important archaeological sites associated with early Christianity.

John the Baptist's settlement is connected with several biblical events including the baptism of Jesus which took place in Bethany, Joshua's crossing of the Jordan River, the last days of Moss, and the Prophet Elijah's crossing of Jordan where he ascended to heaven in a whirlwind upon a chariot with horses of fire (2 Kings 2:5-14). For nearly 2000 years, local church traditions and pilgrimages have identifiedy the small hill at the center of Bethany as the site from which Elijah was raised to paradise. The site became famous for this hill, Elijah's Hill (also Tell Mar Elias, Jabal Mar Elias), which is located 2km west of the Jordan River

The settlement of Bethany and surrounding regions in Jordan has been known by various names throughout history including Ainon, Saphaphas, Bethanin, and Bethabra (Beit el-Obour, or house of the crossing), Arabic language bibles refer to it as Beit' Anya. Thus, today the entire region that falls between Bethany and the Jordan River is called El-Maghtas (the place of immersion or baptism).

Current archaeological studies in the area have identified numerous structures, including monastic complexes, churches, caves, and a system of water pipes, and channels as well as other facilities from the Roman and Byzantine era (4^{th} to 8^{th} centuries AD) (Waheeb 2001). Effectively, these excavations have revealed a settlement from the time of Jesus and John the Baptist (early 1^{st} century AD).

The existence of excavated water structures, such as aqueducts, pools, cisterns, and pottery pipes, attests to the complexity of the water system in the area. Previously settlers had depended on rainwater catchments and springs as sources of water, prompting the Roman and Byzantine to divert water from nearby Wadi using conduit and pottery pipes to fill pools and cisterns as reservoirs (Waheeb 2003).

3 GPR concepts

Ground-penetrating radar (GPR) is a high-resolution method of imaging subsurface structures using electromagnetic (EM) waves with a frequency band from 10 MHz to 1 GHz. The benefit of using (EM) waves is that signals of a relatively short wavelength that can be generated and directed to the subsurface to map anomalous vary in their electrical properties, in many aspects.

The horizontal resolution links to the ability to detect reflector location in space or time, which is a function of the pulse width. The vertical resolution increases with an increase in the frequency. The vertical resolution is also controlled by wavelength (λ) (Knapp, 1990), which is a function of velocity and frequency:

$$\lambda = v/ f$$

The best vertical resolution can be obtained by using one-quarter of the dominant wavelength (Sheriff 1977).

4 GPR Survey

A continuous GPR survey was conducted utilizing a SIRvoyer-20, produced by Geophysical Survey Systems, Inc. (GSSI). 900 MHz and 400 MHz frequency antennas were used in this study. A total of 88 meters of GPR surveys were conducted along eleven profiles at three different locations. The first survey location is located to the north of John the Baptist Church, the second is locate to the south of the pools, and the third location is at Elijah's Hill.

Three profiles were conducted at each of the first two locations and five additional profiles were carried out on the south side of at the third location at Elijah's Hill (Fig. 1). At the second and third sites, the surveys used a 900 MHz antenna.

4.1 Data processing

Minimum data processing was applied to utilize the GSSI RADAN V software package from GSSI. Horizontal and vertical high and low pass filters have been applied to enhance the radar cross-section and to eliminate the surplus noise from the GPR signal. Additional processing to convert two-way travel times along the section to depth in meter applying average radar wave velocity. Data were stacked in the horizontal direction along with profiles. The Data then edited while both horizontal and vertical scales were attuned before processing (Abueladas, 2005).

Time-zero correction was applied to the raw GPR data, which were then managed using range and display gain, filtering, color conversion, and migration procedures (Aqeel et al. .2014).

The GPR data, that were obtained, were processed and presented as 2-D depth cross-sections providing a logical vertical/horizontal resolution for the uppermost 2 m of the inspected sites (Odah et al., 2013). Calculation of the subsurface radar-wave velocity is essential to convert the two way travel time (TWT) of the reflected signal to the real depth of the reflector (Annan 2003; Fisher et al. 1992). However, this study calibrated the velocity according to the known depth aligned with the top of the excavated pipe near the study area.

The dielectric permittivity of the various areas was obtained using an approximation of the reflection delay formula, which connects wave velocity (v), to measured depth (x), the recorded two-way travel time (t), the relative permittivity (ε_r), and the free-space velocity (c) (Gracia et al. 2008)

$$\varepsilon_r = \left(\frac{c}{v}\right)^2 = \left(\frac{ct}{2x}\right)^2$$

The computed near-surface average velocity was 0.12 m/ns (Fig. 2).

Figure 2

5 Results and discussion

Because the lack of geophysical and archaeological data for the study area, therefore it was too difficult to interpret the GPR data.

A total of three continuous parallel profiles up to 12 m long were recorded at site number The separation between the adjacent west-east profiles is constant at 1 m (Fig. 1).

The 400 MHz antenna radar gram along profile 4001 shows a large discontinuous linear discontinuous anomaly at approximate depth of 1.2 m that is interpreted as a discontinuous buried wall and can be viewed in figure 3.

Figure 3

Profile 4002, which is located 1m to the north, shows the same anomaly that was observed in profile 4001; however it was detected at shallower depth (Fig. 4).

These anomalies are caused by dissimilarities in wave velocity at the point of contact between disparate materials. Their depths and extensions of these anomalies most likely indicate the possibility that buried wall with a north-south orientation is presented in subsurface. No other anomalies were detected within profile 4003.

Figure-4

A 900 MHz antenna with good spatial resolution was used at sites 2 and 3 and repeated. GPR survey was performed along the profiles to provide more information about subsurface structures.

A 900 MHz antenna survey was conducted at site 2 along profile 9001from west to east (Fig. 1). Figure 5 shows one primary anomaly at a depth of 0.25 m, located between the 1 m and 3m markers that is interpreted as a buried wall. The 3-meter-wide depression at the end of the profile may be correlated to a shallow buried channel.

Figure-5

Profile 9002 is 10 m long and runs parallel to profile 9001, approximately 1 m to the north (Fig. 1). The same anomaly and depression were detected along this profile as were found in profile 9001 (Fig. 6).

Figure-6

The 12 m long profile 9003 is located to the north of profile 9002 closer to the pool (Fig. 1). The radar profile shows an anomaly between the 2 m and 5 m markers at an approximate depth of 0.25 m, which is interpreted as a buried wall (Fig. 7). The bottom of the depression along this profile is deeper, and the width is lesser than profiles to the south.

Figure-7

Site 3 is a 2 by 5 m a rectangular section on a flat area near Elijah's Hill. The uni-directional survey was conducted along five profiles oriented approximately north-south and spaced 0.5 m apart to the east of the excavated section of pottery pipe (Fig. 1).

The pottery pipe is one of the structures associated with an ancient water system. Most sections of this pipe were destroyed by human activities, but an intact segment was successfully excavated within the site.

GPR profile 1 was collected perpendicular to the trend of the excavated pottery pipe just east of the excavation using a 900 MHz antenna (Fig. 1). The hyperbolic-shaped anomaly appears at the 2.5 m mark, and is about 0.55 m deep showing the location of the buried pipe (Fig. 8).

Figure-8

The main anomalies appear as diffraction hyperbolas with high amplitudes, observed at the 2.5 m marker and at 0.55 m depth, along the entirety of the 2D ground-penetrating radar cross-section.

Generally, targets of interest are easier to identify using three-dimensional data rather than conventional two-dimensional profile lines. The 3D GPR data were generated from

2D and displayed using 3D-visualisation techniques, which is of primary importance in archaeological applications.

A 3D perspective view of the processed profiles using high pass and low pass vertical and horizontal filters together with the migration technique illustrates the location of the pottery pipe (Fig. 9) (Whiting 2001; Fisher et al. 1992a).

Figure-9

Depth slices which are useful for accurate interpretation were generated at different depths (0, 0.25, 0.55, 0.75 m) from the 3D plot are presented in figure 10. The main anomaly observed on the depth slice of 0.55 mbs (meter below the surface) has a west-east orientation and corresponds to the pottery pipe anomaly, which provides good information about the exact location and extension of the pipe.

Figure-10

The multiple slices view along the y-direction at various distances (0, 1, and 2 m) determines the extension of the pipe anomaly along the y-direction (Fig. 11).

Figure-11

The 3D section (chair view) with X= 2.5 m, Y= 0.85 m, and Z= 0.55 m shows clearly the east-wesr extension of the pipe perpendicular to the X position, and the depth to the top of the pipe determined by the Z position (Fig. 12). The results of this study showed that many subsurface structures were recognized using GPR. Subsurface walls were delineated and various subsurface channels were found.

Figure-12

The locations of these channels were well defined and flow directions in these channels were also identified from west to east in the study area. Fig. 13 shows the location map of GPR anomalies and their interpretation.

Figure-13

6 Conclusions

Ground-penetrating radar (GPR) is a powerful, non-destructive, non-invasive geophysical near-surface tool for archaeological surveying. GPR has been used successfully in this study to detect several shallow anomalies at El-Maghtas Site. The flat topography and the absence of archaeological features at the surface of the site allowed for collection of good quality GPR data. The high frequency 900 MHz antenna was used successfully to locate smaller archaeological objects at shallow depths and 3D images provided high resolution than the 2D profiles, as can be seen from the results. Generally, the survey included the identification and mapping of covered walls, channels, and the extension of an ancient pottery pipe.

However, vertical sections, depth slices, and 3D images were used to locate the anomalies using spatial extent 3D survey, allowing for a precise detection of the anomaly throughout the surveyed data after advanced processing, including migration. The east-west oriented extension of the pottery pipe in the El-Maghtas site was detected successfully by using three-dimensional GPR imaging.

The mapped archaeological targets are relatively shallow, showing detectable anomalies from approximately 0.55 m below the ground surface extending to a depth of 1.2 m.

The displacement shown in the buried wall and channel in site 2 may be caused by a shallow fault. The results of this study can be used as a source for any future excavations.

Acknowledgments

The authors would thank the Ministry of Higher Education and Scientific Research for their fund and support throughout the project. We would also like to thank Eng. B. El-Madani, the former Baptism site Commission Director and his assistant Eng R. Mkhjian for their help. We are also grateful to the technicians, I. Aldabas, M. Aqrabawi, Z. Heyassat the employees of (BAU) for their efforts during data acquisition in the fieldwork. We thank the anonymous reviewers and the editor for their constructive critics and comments on this manuscript very much.

References

Abueladas, A.: Ground Penetrating Radar Investigations of Active Faults and Antiquities along the Dead Sea Transform in Aqaba and Taba Sabkha, Jordan, master thesis, University of Missouri-Kansas City, U.S.A, 71 pp., 2005.

Annan, AP.: GPR principles, procedures and applications: Sensors and Software In, 2003.

Aqeel, A., Anderson, N., and Maerz, N.: Mapping sub-vertical discontinuities in rock cuts using a 400-MHz ground penetrating radar antenna, Arab J Geosci 7(5), 2093–2105, https://doi.org/10.1007/s12517-013-0937-y, 2014.

Basile, L., Carrozzo, MT, Negri, S., Nuzzo, S., Quarta, L., and Villani, A.V.: A ground-penetrating radar survey for Archaeological investigations in an urban area (Lecce, Italy), Journal of Applied Geophysics, 44, 15-32, https://doi.org/10.1016/S0926-9851(99)00070-1, 2000.

Cacione, JM.: Radar simulation for archaeological applications: Geophysical Prospecting, 44, 871-888, https://doi.org/10.1111/j.1365-2478.1996.tb00178.x, 1996.

Eppelbaum, L.V., and Khesin, B.E.: Disturbing factors in geophysical investigations at archaeological sites and ways of their elimination. In: Transactions of the IV Conference on Archaeological Prospection, Vienna, Austria, 19-23 September 2001, 99–10, 2001

Eppelbaum, L.V., Khesin, B.E. and Itkis, S.E.: Archaeological geophysics in arid environments: Examples from Israel, Journal of Arid Environments, 74, 849-860, https://doi.org/10.1016/j.jaridenv.2009.04.018, 2010.

Gracia, V., Garcı, F., Pujades, L., Drigo, R., and Capua, D.: GPR survey to study the restoration of a Roman monument, Journal of Cultural Heritage, 9, 89-96, https://doi.org/10.1016/j.culher.2007.09.003, , 2008.

Fisher, E.: Examples of reverse-time migration of single-channel, ground penetrating radar profiles. Geophysics, 57, 577-586, https://doi.org/10.1190/1.1443271, 2006.

Knapp, R. W.: Vertical resolution of thick beds, thin beds and thin-bed cyclothems, Geophysics, 55, 1183-119, https://doi.org/10.1190/1.1442934, 1990.

Neal, A.: Ground-penetrating radar and its use in sedimentology: principles, problems and progress, Earth-Science Reviews, 6, 261–330, https://doi.org/10.1016/j.earscirev.2004.01.004, 2004.

Odah, H., Ismail, A., Elhemaly, I., Anderson, N., Abbas, A., and Shaaban, F.: Archaeological exploration using magnetic and GPR methods at the first court of Hatshepsut Temple in Luxor, Egypt, Arab J. Geosci, , 6, 865–871, https://doi.org/10.1007/s12517-011-0380-x, 2014.

Ronen A, Ezersky M, Beck A., Gat enio B., Simhayov R.B (2018) Use of GPR method for prediction of sinkholes formation along the Dead Sea Shores, Israel. Geomorphology 328: 28-43. https://doi.org/10.1016/j.geomorph.2018.11.030

Sheriff, R. E., and Geldart, L. P.: Reflection field methods, Cambridge University Press, England, 1995.

Sternberg, B. K., McGill, J. W.: Archaeology studies in southern Arizona using ground penetrating radar. Journal of Applied Geophysics, 33, 209-225, https://doi.org/10.1016/0926-9851(95)90042-X, 1995.

Vaughan C. J.: Ground penetrating radar survey used in archaeological investigations. Geophysics, 51, 595-604, https://doi.org/10.1190/1.1442114., 1986.

Waheeb, M (2003) Recent Discoveries in the Bethany Beyond Jordan in Jordan Valley. ADAJ 47:243-246.

Waheeb M (2001) Archaeological Excavations at the Baptism Site, Bethany Beyond the Jordan. Bible and Spade 14(2):43-53.

Whiting, B, McFarland, D., and Hackenberger, S.: Thee-Dimensional GPR study of a prehistoric site in Barbados, West Indies. Journal of Applied Geophysics, 47, 217-226, https://doi.org/10.1016/S0926-9851(01)00066-0, 2001.

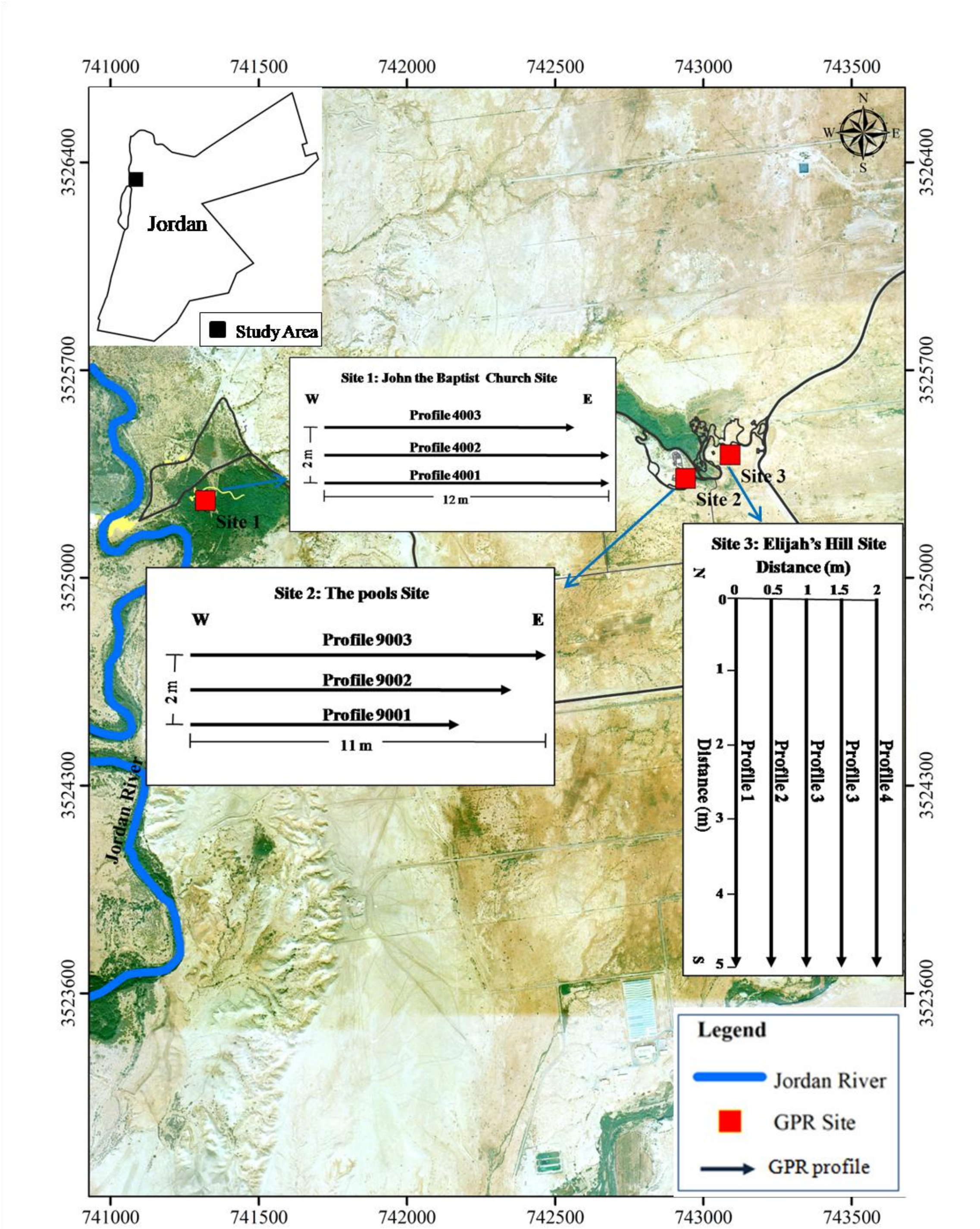
741000
741500
742000
742500
743000
743500
3526400
3525700
3525000
3524300
3523600
Jordan
Study Area
N
S
W
E
Site 1: John the Baptist Church Site
W
E
Profile 4003
Profile 4002
Profile 4001
2 m
12 m
Site 1
Site 2
Site 3
Site 2: The pools Site
W
E
Profile 9003
Profile 9002
Profile 9001
2 m
11 m
Site 3: Elijah's Hill Site
Distance (m)
0
0.5
1
1.5
2
1
2
3
4
5
Distance (m)
Profile 1
Profile 2
Profile 3
Profile 3
Profile 4
Jordan River
Legend
Jordan River
GPR Site
GPR profile

Figure-1

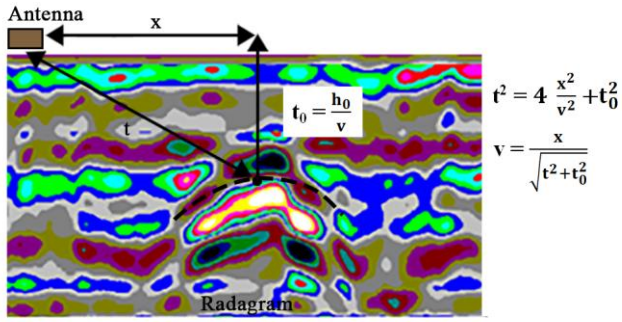
Antenna
x
t
$t_0 = \frac{h_0}{v}$
$t^2 = 4\ \frac{x^2}{v^2} + t_0^2$
$v = \frac{x}{\sqrt{t^2 + t_0^2}}$
Radagram

Figure-2

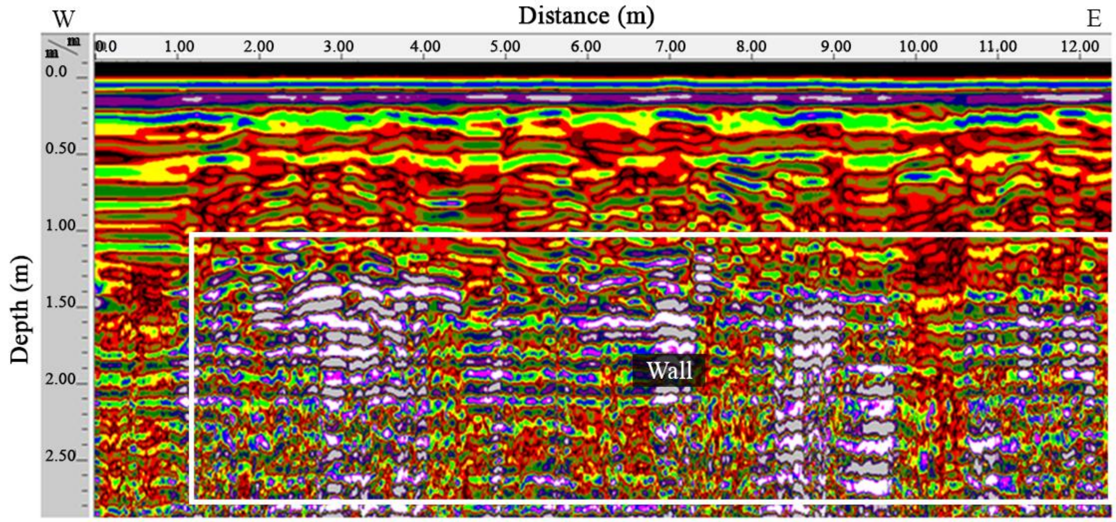
W
Distance (m)
E
0.0
1.00
2.00
3.00
4.00
5.00
6.00
7.00
8.00
9.00
10.00
11.00
12.00
0.50
1.50
2.50
Depth (m)
Wall

Figure-3

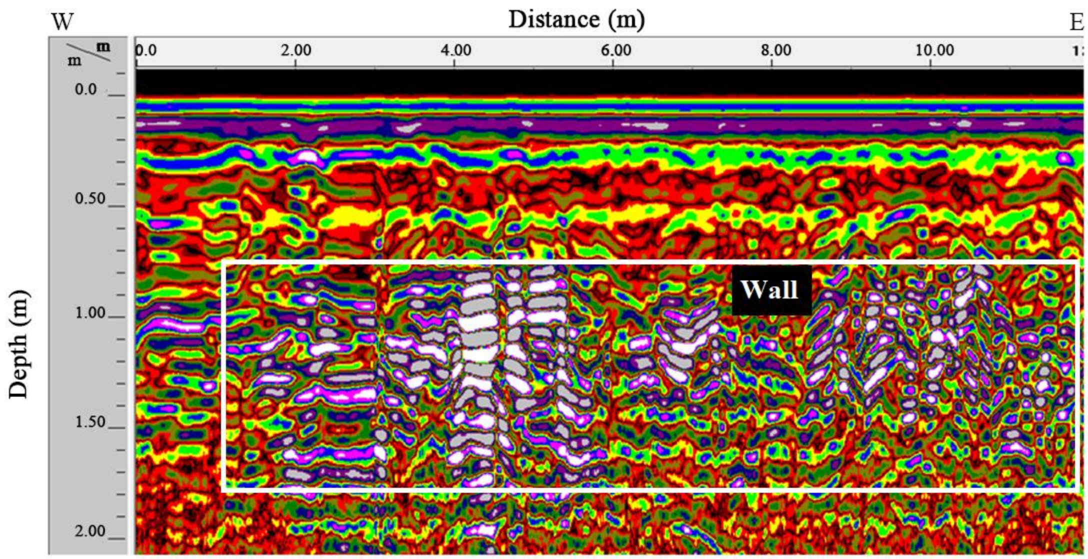
W
Distance (m)
E
0.0
2.00
4.00
6.00
8.00
10.00
0.0
0.50
1.00
1.50
2.00
Depth (m)
Wall

Figure-4

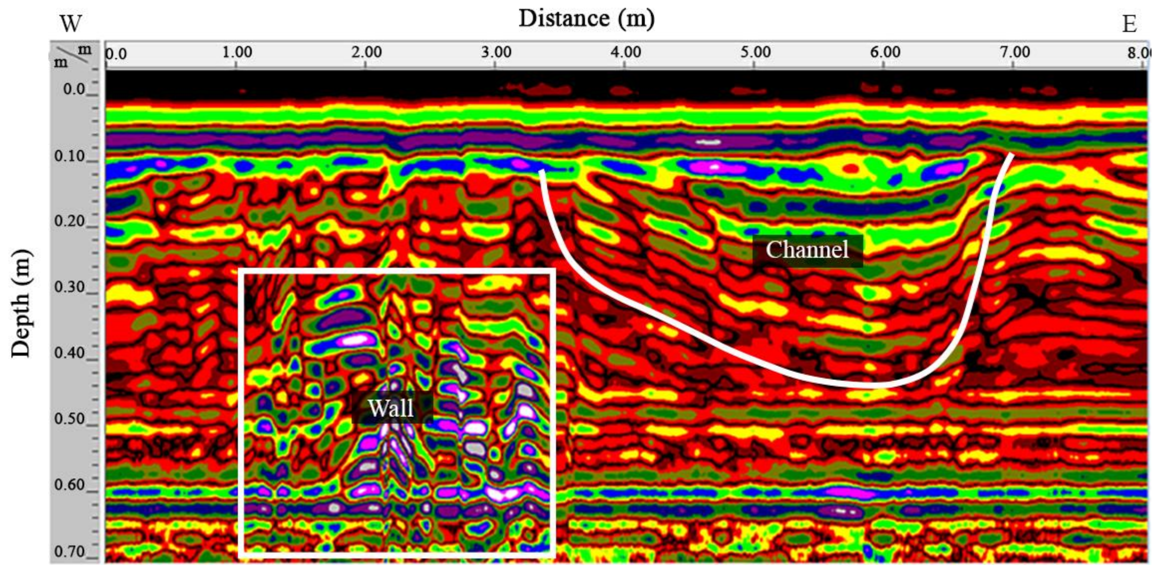
W
Distance (m)
E
0.0
1.00
2.00
3.00
4.00
5.00
6.00
7.00
Depth (m)
0.10
0.20
0.30
0.40
0.50
0.60
0.70
Channel
Wall

Figure-5

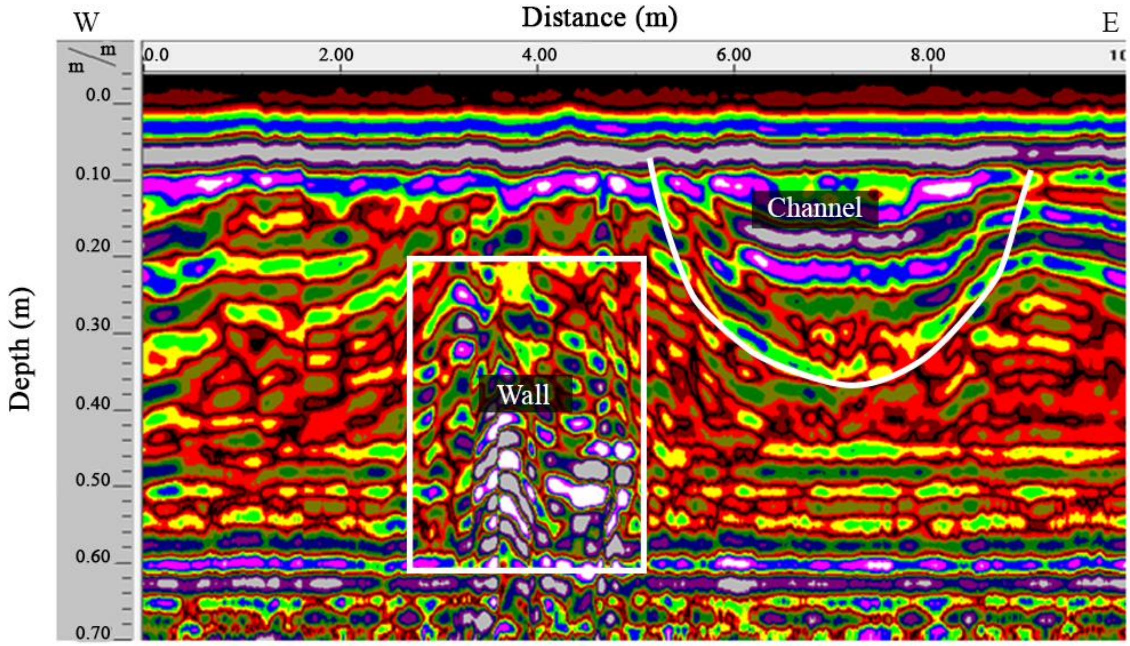
W
Distance (m)
E
0.0
2.00
4.00
6.00
8.00
Depth (m)
0.0
0.10
0.20
0.30
0.40
0.50
0.60
0.70
Channel
Wall

Figure-6

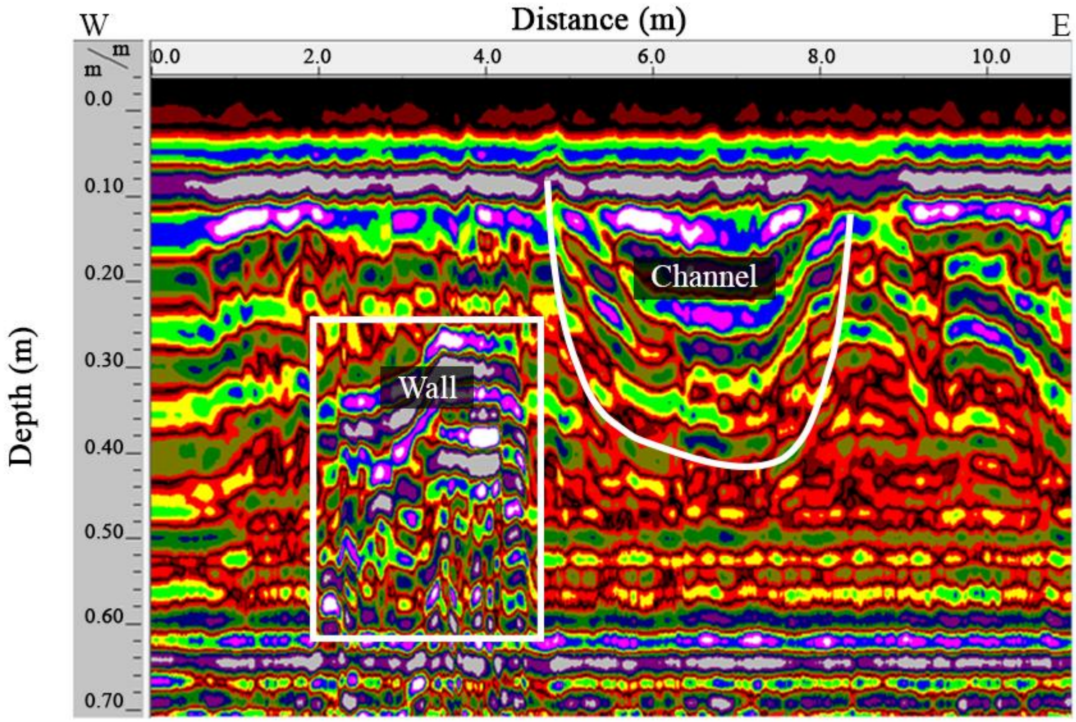
W
Distance (m)
E
m
m
0.0
2.0
4.0
6.0
8.0
10.0
0.0
0.10
0.20
0.30
0.40
0.50
0.60
0.70
Depth (m)
Channel
Wall

Figure-7

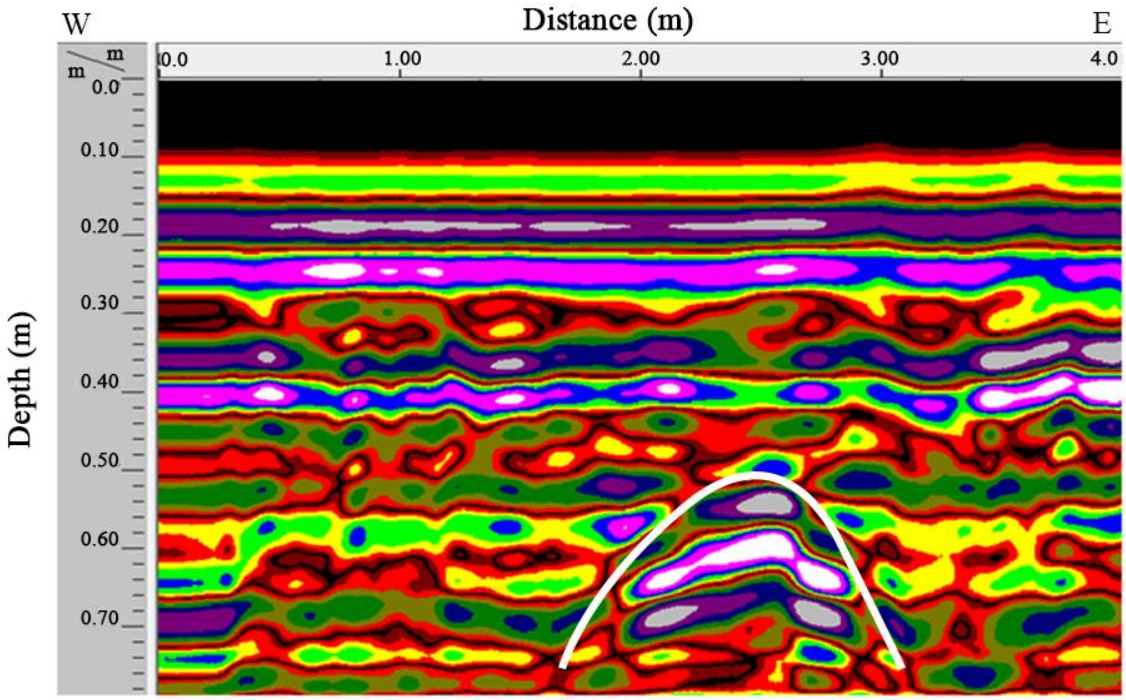
W
Distance (m)
E
m
m
0.0
1.00
2.00
3.00
4.0
0.0
0.10
0.20
0.30
0.40
0.50
0.60
0.70
Depth (m)

Figure-8

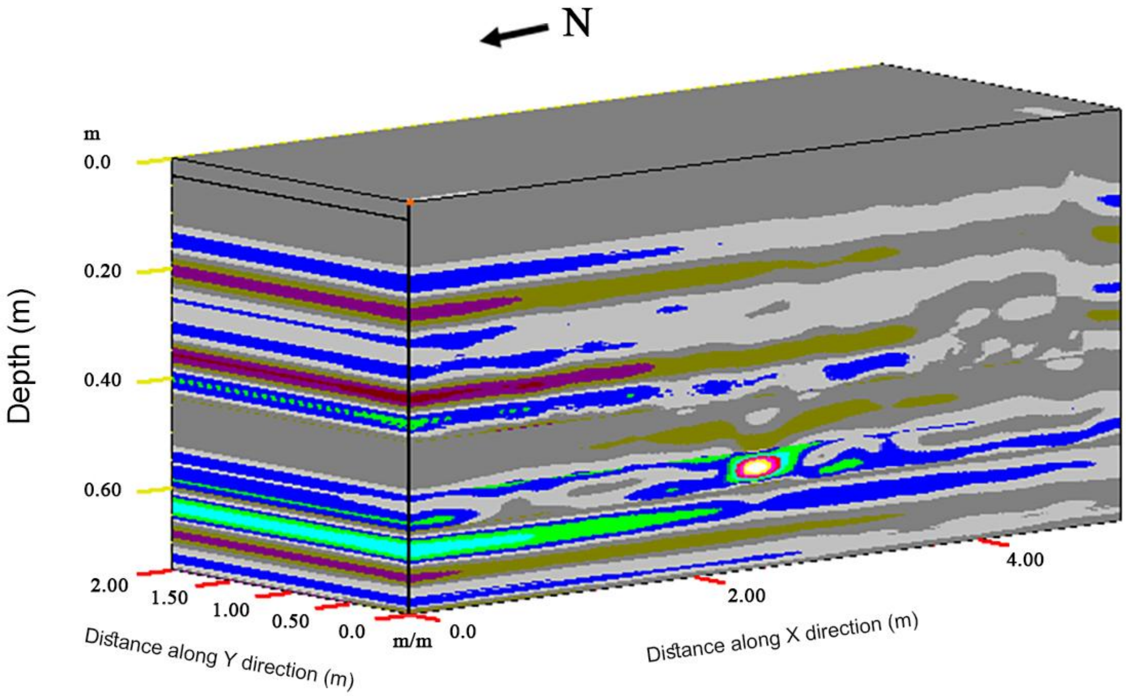

N
m
0.0
0.20
0.40
0.60
Depth (m)
2.00
1.50
1.00
0.50
0.0
m/m
0.0
2.00
4.00
Distance along Y direction (m)
Distance along X direction (m)

Figure-9

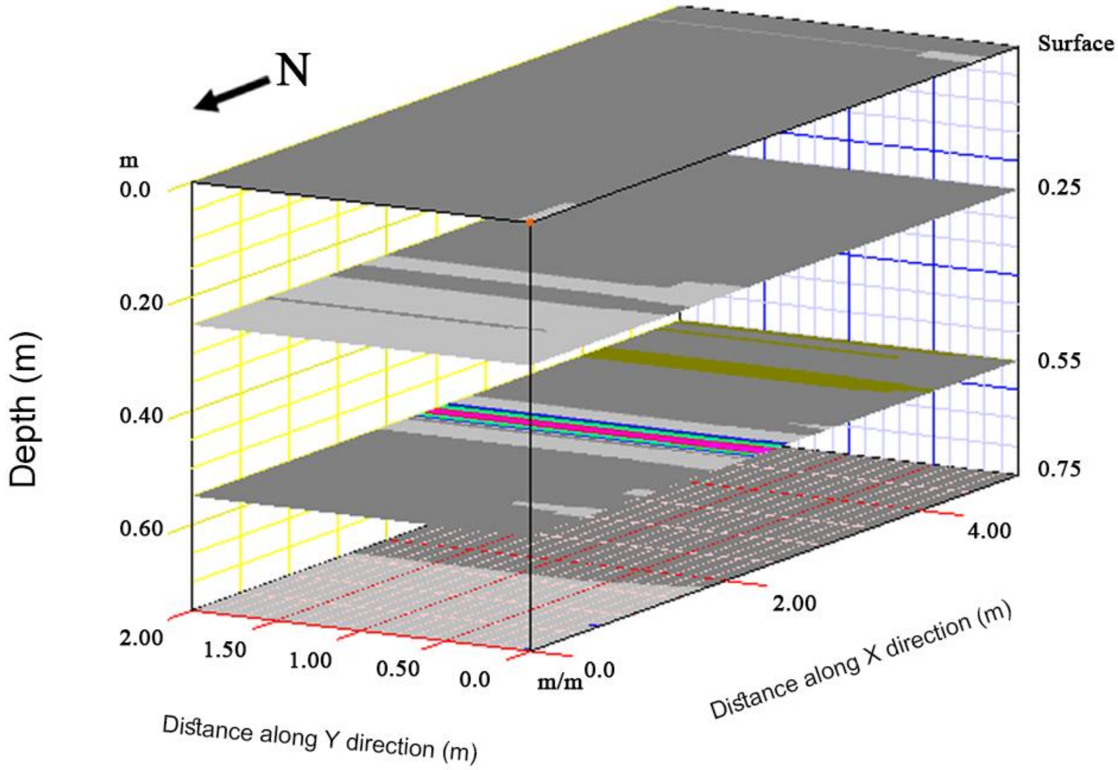
N
m
0.0
0.20
0.40
0.60
2.00
Depth (m)
Surface
0.25
0.55
0.75
4.00
2.00
1.50
1.00
0.50
0.0
m/m
0.0
Distance along Y direction (m)
Distance along X direction (m)

Figure-10

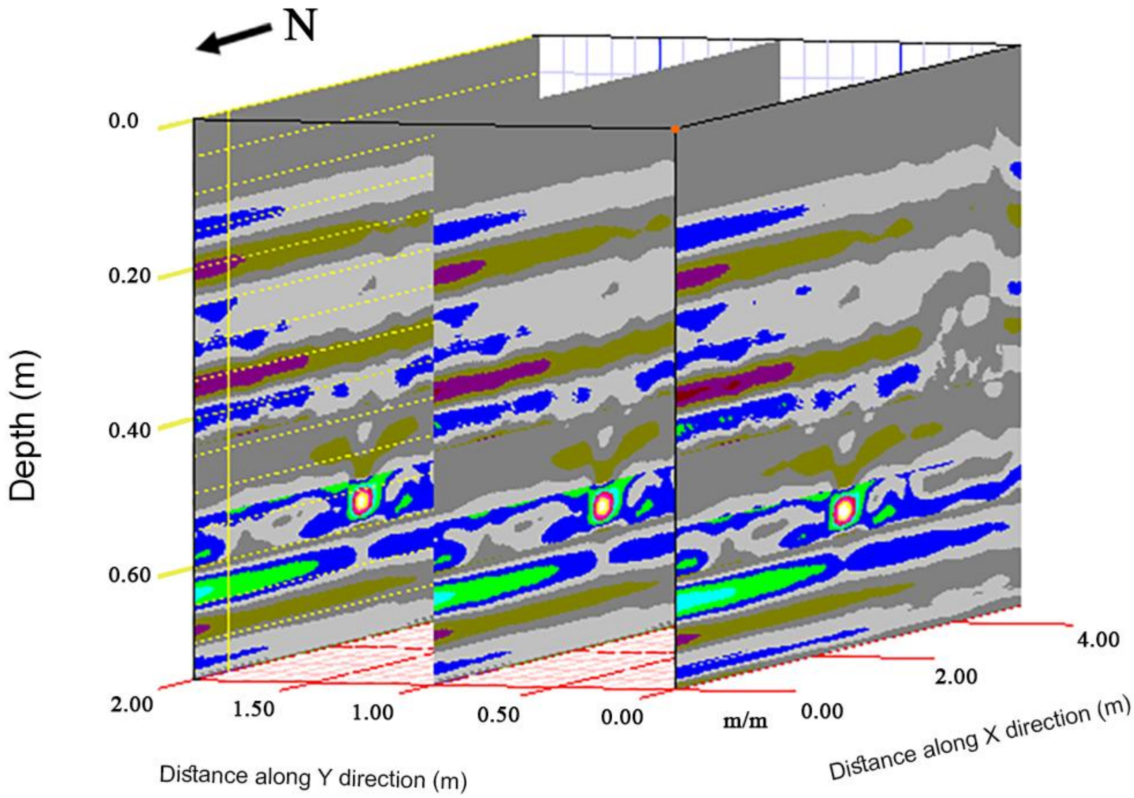
N
Depth (m)
0.0
0.20
0.40
0.60
2.00
1.50
1.00
0.50
0.00
m/m
0.00
2.00
4.00
Distance along Y direction (m)
Distance along X direction (m)

Figure-11

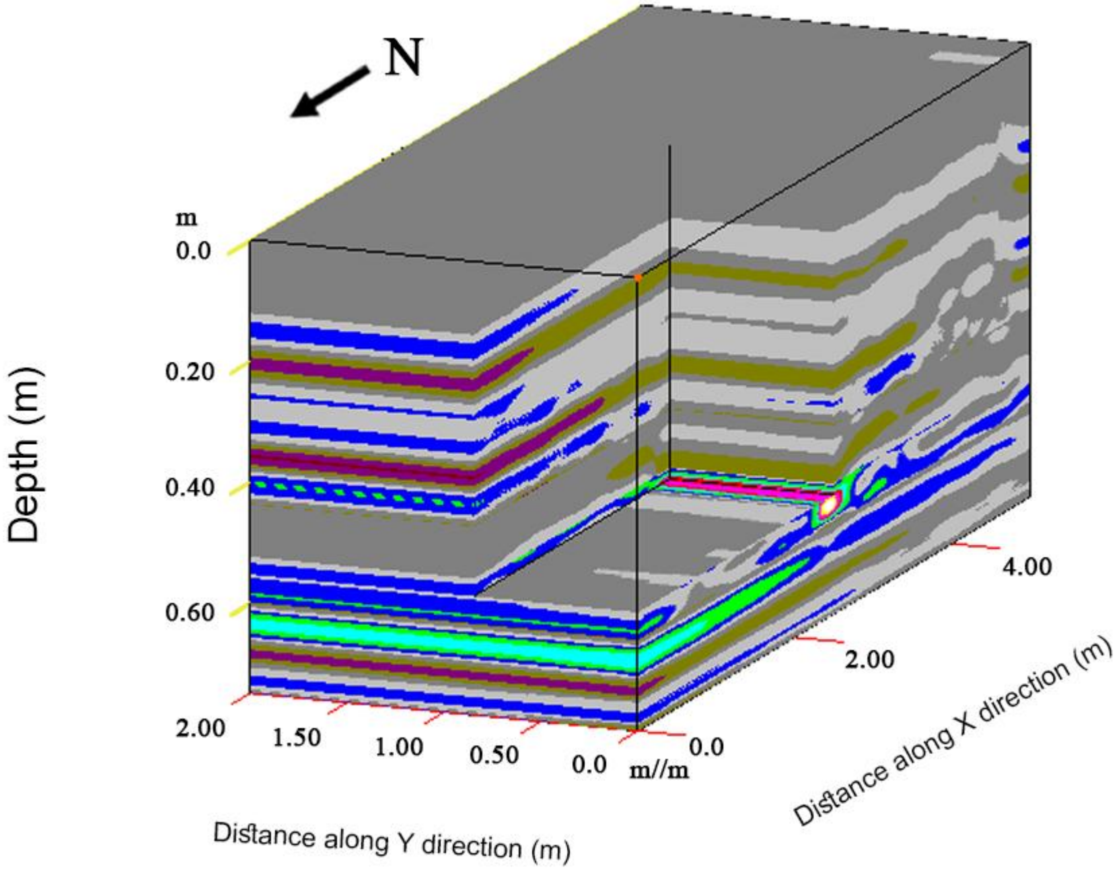
N
m
0.0
0.20
0.40
0.60
Depth (m)
2.00
1.50
1.00
0.50
0.0
m//m
0.0
2.00
4.00
Distance along X direction (m)
Distance along Y direction (m)

Figure-12

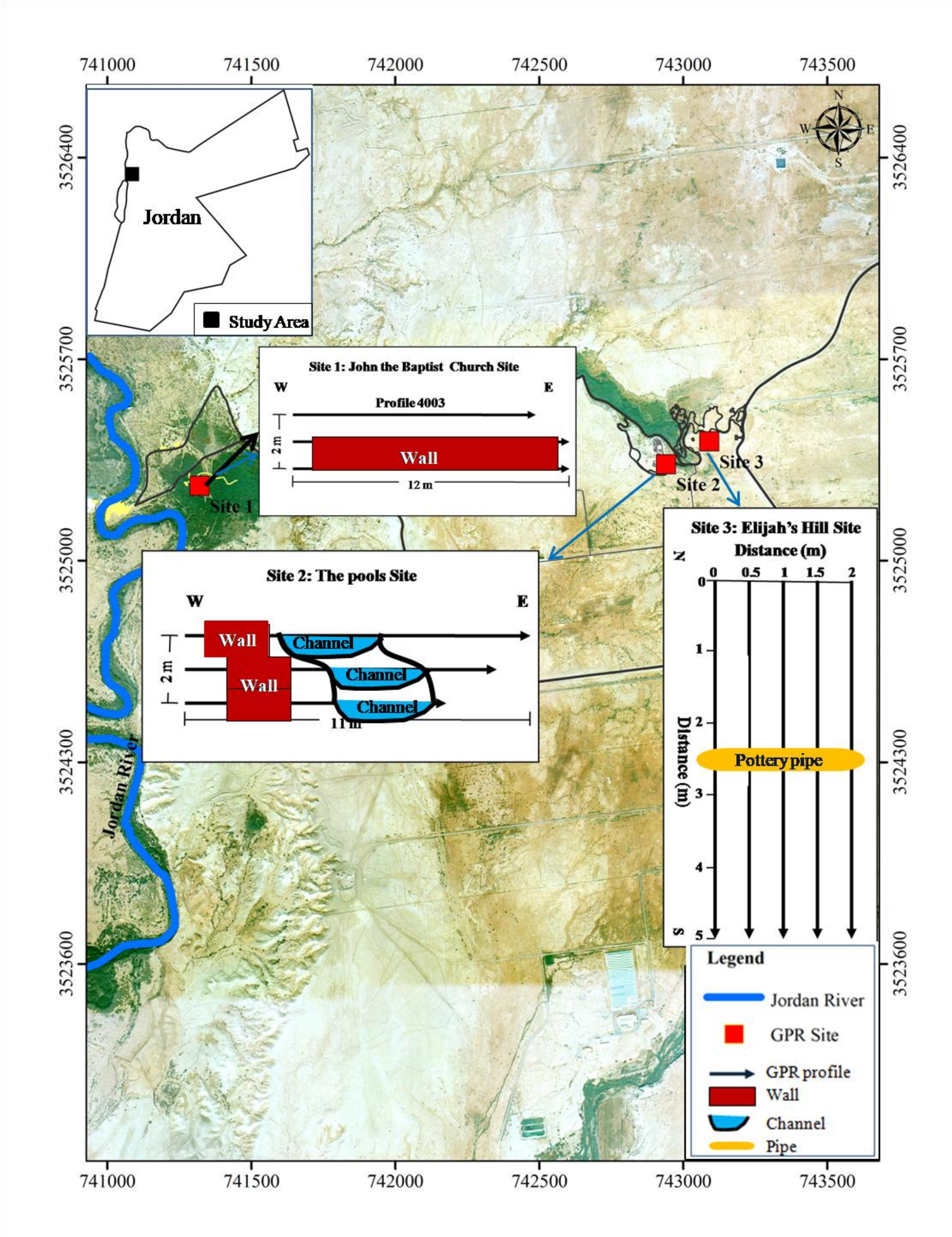

Figure-13

Figures Captures

Fig.1. Location map of the GPR profiles study area (After Google Earth).

Fig.2. Hyperbolic reflections caused by pottery pipe is used to obtain the wave velocity with the equation of hyperbola.

Fig.3. A 400 MHz antenna radargram along Profile4001. The white rectangle along the radargram at approximate depth of 1.2 m may correspond to buried wall.

Fig.4. A 400 MHz antenna radargram along Profile4002. The white rectangle along the radargram at approximate depth of 0.6 m may correspond to buried wall.

Fig.5. A 900 MHz antenna radargram along Profile9001. The white rectangle along the radargram represents anomaly located between horizontal distance 1 and 3 m with approximate depth 0.25 m which may correspond toan ancient buried wall. The 4 m wide depression at end of the profile may be correlated to buried channel.

Fig.6. A 900 MHz antenna radargram along Profile9002. The white rectangle along the radargram at approximate depth of 0.20 m may correspond to buried wall. The 4 m wide depression at end of the profile may be correlated to buried channel.

Fig.7. A 900 MHz antenna radargram along Profile9003. The white rectangle along the radargram at approximate depth of 0.20 m may correspond to buried wall. The 4 m wide depression at end of the profile may be correlated to buried channel.

Fig. 8 A part of 900 MHz antennae radargram along profile 1 immediately adjacent to excavated pottery pipe. The hyperbolic- shaped anomaly at distance 2.5 m and 0.55 m deep shows the extension location of the buried pottery pipe.

Fig. 9 The 3D GPR data view constructed from 2D profile lines. The 3D perspective view of processed profiles using high pass and low pass vertical and horizontal filters together with migration technique that show the location of the pottery pipe.

Fig.10. Depth slices with different depths (0, 025, 0,55, 0.75 m) generated from 3D plot . The main anomaly observed with W-E direction at depth slice 0.55 mbs (meter below surface).

Fig.11. The multiple slices view along y direction at distance (0, 1 and 2 m) determines the depth and extension of the pipe.

Fig.12. The 3D section (cutout cube) using X=2.5 m,Y=0.85 m, and Z=0.55 m shows clearly the depth and extension of the pipe perpendicular to the X position and the depth of the top of pipe detect by the Z position.

Fig.13. Location map of the inferred archaeological material (after Google Earth)